Eur J Nucl Med Mol Imaging (2012) 39:416–420
DOI 10.1007/s00259-011-1985-8

SHORT COMMUNICATION

Microvascular dysfunction in nonfailing arrhythmogenic right ventricular cardiomyopathy

Matthias Paul · Kambiz Rahbar · Joachim Gerss · Peter Kies · Otmar Schober · Klaus Schäfers · Günter Breithardt · Eric Schulze-Bahr · Thomas Wichter · Michael Schäfers

Received: 5 August 2011 / Accepted: 21 October 2011 / Published online: 24 November 2011

Abstract
Purpose Arrhythmogenic right ventricular cardiomyopathy (ARVC) is a nonischaemic cardiomyopathy and leading cause of sudden death in the young. It has been shown that microvascular dysfunction reflected by an impaired myocardial blood flow (MBF) response to stress is present in patients with other forms of nonischaemic cardiomyopathy, e.g. dilated cardiomyopathy, and that the reduced MBF may be related to a poor prognosis. Therefore, we quantified MBF, coronary flow reserve and coronary vascular resistance in patients with non-failing ARVC using $H_2{}^{15}O$ and PET.
Methods In ten male patients with ARVC (mean age 49±14 years), MBF was quantified at rest and during adenosine-induced hyperaemia using $H_2{}^{15}O$ PET. Results were compared with those obtained in 20 age-matched healthy male control subjects (mean age 46±14 years).
Results Resting MBF was not significantly different between patients with ARVC and controls (MBF_{rest} 1.19±0.29 vs. 1.12±0.20 ml/min/ml). However, hyperaemic MBF was significantly lower in patients with ARVC than in controls (2.60±0.96 vs. 3.68±0.84 ml/min/ml; $p=0.005$). Consequently, patients with ARVC had a significantly lower coronary flow reserve than control subjects (2.41±1.34 vs. 3.39±0.93; $p=0.030$). In addition, hyperaemic coronary vascular resistance was increased in patients with ARVC (36.79±12.91 vs. 26.31±6.49 $mmHg \times ml^{-1} \times min \times ml$; $p=0.007$), but was found to be unchanged at rest.
Conclusion In this small well-characterized cohort of patients with nonfailing ARVC, we found a significantly reduced hyperaemic MBF and increased coronary vascular resistance. Further studies are necessary to corroborate this potential new functional aspect of the pathophysiological mechanisms underlying ARVC.

Keywords Arrhythmogenic right ventricular cardiomyopathy · Myocardial perfusion · Myocardial blood flow · Coronary vascular resistance · Positron emission tomography

Matthias Paul and Kambiz Rahbar contributed equally to this work.

M. Paul (✉) · G. Breithardt
Department of Cardiology and Angiology,
University Hospital Münster,
Albert-Schweitzer-Campus 1 – Gebäude A1,
48149 Münster, Germany
e-mail: Matthias.Paul@ukmuenster.de

M. Paul · E. Schulze-Bahr
Institute for Genetics of Heart Diseases,
University Hospital Münster,
Münster, Germany

K. Rahbar · P. Kies · O. Schober
Department of Nuclear Medicine, University Hospital Münster,
Münster, Germany

J. Gerss
Institute of Biostatistics and Clinical Research,
University of Münster,
Münster, Germany

K. Schäfers · M. Schäfers
European Institute for Molecular Imaging – EIMI,
University of Münster,
Münster, Germany

T. Wichter
Department of Cardiology, Niels-Stensen-Kliniken,
Marienhospital Osnabrück,
Osnabrück, Germany

Introduction

Arrhythmogenic right ventricular cardiomyopathy (ARVC) is a myocardial disease frequently associated with recurrent ventricular tachycardia and sudden cardiac death in a young population [1]. Studies of the myocardial sympathetic nervous system in patients with ARVC have revealed left ventricular involvement [2] which could result in an impairment of vascular reactivity. In addition, microvascular dysfunction has been detected in patients with other non-ischaemic cardiomyopathies, in whom it is an independent predictor of clinical deterioration and death [3, 4]. Therefore, we investigated myocardial perfusion reserve in patients with ARVC.

Methods

Study population

Ten male patients with well-characterized definite ARVC (49±14 years) were prospectively enrolled in this study. The diagnosis of ARVC was established in accordance with the proposed diagnostic criteria [1] with major criteria counting as 2 and minor criteria as 1 score point. At least 4 points from different diagnostic groups were required for the diagnosis of ARVC. None of the study patients had hypertension, clinical signs or symptoms of coronary artery disease, or heart failure.

All patients underwent detailed noninvasive (12-lead ECG at rest and two-dimensional transthoracic echocardiography) and invasive investigations (including right/left ventriculography and coronary angiography). Upon transthoracic echocardiography, left ventricular end-diastolic and end-systolic diameters were measured in the parasternal long axis view and indexed to the body surface area. In addition, fractional shortening was used to evaluate left ventricular function. All aforementioned parameters were calculated without knowledge of the PET results according to published recommendations [5], and were normal in all patients (Table 1) with no evidence of valvular stenoses or higher degree of valvular regurgitation. Patients and controls alike were in sinus rhythm. Thyroid disease, diabetes mellitus and familial hypercholesterolaemia were excluded prior to the PET scan. The clinical characteristics of the patients are summarized in Table 1.

Control group

The control group comprised 20 healthy age- and sex-matched subjects (46±14 years) without structural heart disease. No control subject had clinical signs or symptoms suggestive of coronary artery disease. In addition, exercise stress tests and two-dimensional transthoracic echocardiography were performed prior to study entry and were normal in all subjects.

All patients and control subjects gave written informed consent to the study protocol approved by the local ethics committee of the Medical Faculty of the University of Münster, Germany.

Table 1 Individual clinical and echocardiographic characteristics of the patients with ARVC

Patient no.	Age (years)	Diagnosis[a]			Body surface area (m^2)	Left ventricular end-diastolic diameter index[b]	Left ventricular end-systolic diameter index[c]	Fractional shortening (%)[d]
		Score	Major criteria	Minor criteria				
1	54	9	4 (A, B, D, F)	1 (E)	1.8	31	16	49
2	55	4	1 (A)	2 (B, E)	2.2	23	13	42
3	51	9	4 (A, B, C, F)	1 (E)	2.1	23	13	48
4	39	8	3 (A, B, F)	2 (C, D)	2.2	21	14	33
5	57	6	2 (A, B)	2 (D, E)	2.2	25	20	30
6	67	6	2 (B, F)	2 (A, C)	1.9	26	16	39
7	28	9	3 (A, B, D)	3 (C, E, F)	1.9	27	17	39
8	24	6	2 (A, F)	2 (C, E)	1.9	25	14	44
9	63	9	3 (A, B, F)	3 (C, D, E)	1.9	27	17	35
10	50	7	3 (A, B, F)	1 (C)	2.4	25	15	41
Mean±SD	49±14	7±2	3±1	2±1	2.1±0.2	25±3	15±2	40±6

[a] According to the modified Task Force criteria [1]. Adapted diagnostic categories: *A* structural alterations, *B* tissue characteristics, *C* repolarization abnormalities, *D* depolarization abnormalities, *E* arrhythmias, *F* family history. See text for details.

[b] Indexed to body surface area; normal range 20–32 mm/m^2.

[c] Indexed to body surface area; normal range 13–21 mm/m^2.

[d] Normal range 25–35%.

Noninvasive measurement of myocardial perfusion in vivo

PET scans were performed after fasting for at least 12 h, particularly in relation to caffeine-containing beverages, chocolate and smoking to avoid interference with adenosine, according to a previously published protocol [6]. In brief, myocardial blood flow (MBF) was assessed after intravenous bolus injection of 500 MBq $H_2{}^{15}O$ over 20 s while performing a 26-frame dynamic PET scan (ECAT-921; Siemens/CTI, Knoxville, TN) over 5 min. The emission data were reconstructed (Hanning filter, FWHM 7.3 mm, zoom factor 2.3, 47 planes, matrix size 128×128). Factor images were generated from the dynamic $H_2{}^{15}O$ scans and resliced into short-axis images perpendicular to the long axis of the left ventricle. This transformation matrix was also used to reslice the dynamic water images. Regions of interest (whole left ventricular myocardium and four-wall analysis) were placed manually on the short-axis planes of the factor images encompassing myocardial tissue, the left atrial cavity and the right ventricular cavity. Arterial, venous and tissue time–activity curves were fitted to a single-compartment model to quantify regional and global MBF (millilitres per minute per millilitre) and perfusable tissue fraction [7]. To eliminate potential interindividual differences in cardiac workload, MBF at rest was corrected for the rate–pressure product (RPP; $MBF_{corrected} = MBF/RPP \times 10{,}000$ [8]). Coronary flow reserve was calculated as the ratio of hyperaemic MBF and the RPP-corrected baseline MBF. Coronary vascular resistance (CVR) was calculated by dividing mean arterial pressure by the respective MBF in different settings (at baseline and under adenosine stress).

Statistical analysis

Data are expressed as means±standard deviation. Student's *t*-tests were used for comparison of continuous variables. The two-sided Spearman's correlation coefficient was calculated to investigate associations between possible confounders and observed outcome data (SPSS, version 16.0 for Windows; SPSS, Chicago, IL). A p-value <0.05 was considered significant.

Results

Resting MBF corrected for the RPP was comparable between patients with ARVC and controls (p=0.42) and not correlated with left ventricular diameter (p=0.197). However, the response of MBF to adenosine was severely blunted in patients with ARVC when compared to controls (p=0.005; Fig. 1) and associated with a lower hyperaemic coronary flow reserve (p=0.030; Fig. 2). Consequently, a significantly increased CVR under hyperaemic conditions was found in patients with ARVC compared to controls (p=0.007; Fig. 3), while baseline CVR was unchanged (p=0.66). In addition, both groups had similar regional

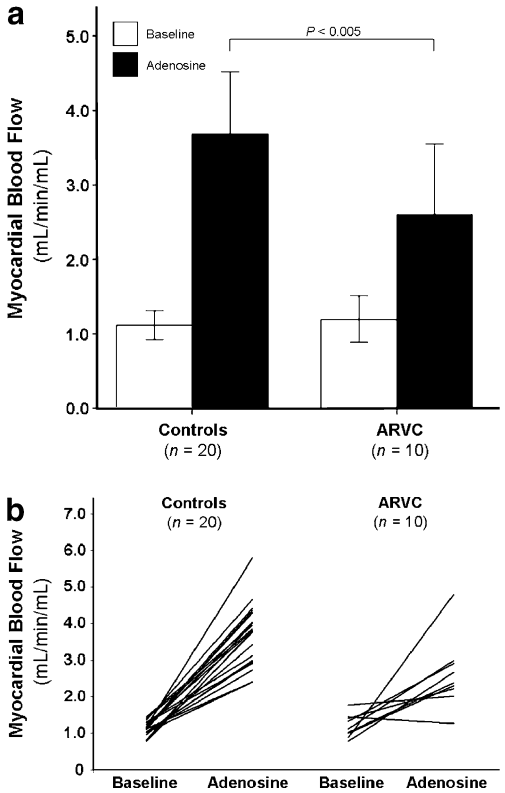

Fig. 1 MBF in patients with ARVC and control subjects as measured by $H_2{}^{15}O$ PET at baseline and under adenosine stress. Baseline MBF is corrected for the RPP. **a** Mean values (±SD) for each group, **b** individual patient results

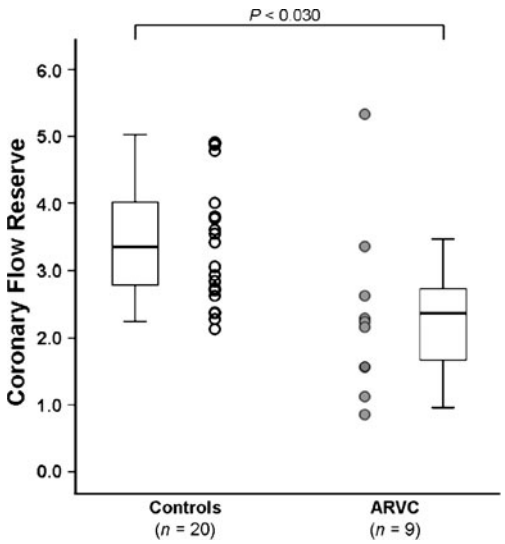

Fig. 2 CFR in patients with ARVC and control subjects (boxplots for the group and scatter plots of individual data)

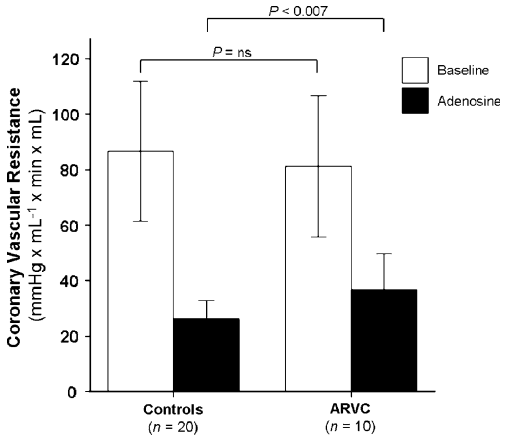

Fig. 3 CVR in patients with ARVC and control subjects as measured by $H_2{}^{15}O$ PET at baseline and under adenosine stress (means ± standard deviation). Baseline CVR is corrected for the RPP

myocardial perfusion patterns at rest and under adenosine stress (data not shown). Importantly, the tissue fraction calculated from the dynamic $H_2{}^{15}O$ PET scans, being a measure of perfusable myocardial tissue in a region-of-interest, was similar between patients with ARVC and controls at baseline (0.65±0.08 g/ml in patients vs. 0.64± 0.07 g/ml in controls; p=0.74), excluding significant myocardial fibrosis in patients with ARVC potentially influencing the quantification of MBF.

Discussion

In the present study investigating microvascular function in well-characterized patients with nonfailing ARVC, we demonstrated for the first time a significantly blunted MBF response to adenosine, which resulted in a decrease in coronary flow reserve of approximately 50% compared to control subjects.

The ratio of MBF during maximal coronary vasodilation to baseline, defined as the coronary flow reserve, is an integrated measure of coronary blood flow through both the large epicardial arteries and the microcirculation, and thus facilitates a functional evaluation of the coronary circulation. Hence, a reduction in coronary flow reserve can result from either angiographically demonstrable coronary artery stenoses, which were ruled out in the study population, or reflect an impairment in coronary microcirculation. Microvascular dysfunction in turn could arise from structural and/or functional impairment on different levels of the coronary arteries – the endothelium, the smooth muscle cells, the autonomic nerves, and others. Since MBF and CVR at baseline were found to be unchanged in our study, impairment of the dilatory responsiveness of the arteries is a likely explanation. Using adenosine to trigger an increase in hyperaemic blood flow allows gross assessment of the endothelium-independent vasodilatory capacity because only a minor fraction of the blood flow increase can be explained by endothelium-dependent mechanisms [9].

Apart from the endothelium-independent vasodilation of microvessels, adenosine infusion typically results in a drop in blood pressure and, in turn, drives the sympathetic tone, as can be seen by an increased heart rate under adenosine stress. In a normal heart this further enhances coronary blood flow through β-adrenoceptor stimulation at the arterial vascular tree resulting in coronary vasodilation at the level of the large artery and arterioles, an effect which "overrides" the parallel α-adrenoceptor-mediated vasoconstriction [10]. However, in a condition such as ARVC, in which MIBG defects and increased washout suggest an impairment of the sympathetic nervous system, this effect might be blunted. Given the inefficiency of the uptake-1 transporter and increased release of catecholamines at the presynaptic sympathetic nerves, the concentration of catecholamines at the synaptic cleft is increased resulting in downregulated β-adrenoceptors. We have previously shown a decrease of about 50% in β-adrenoceptor density in patients with ARVC using ^{11}C-CGP 12177 PET [11]. Downregulation of β-adrenoceptors would in turn result in a blunted β-adrenoceptor-mediated flow response to an adenosine-stimulated increased sympathetic tone while α-adrenoceptor-mediated vasoconstriction is preserved, impairing the maximal MBF under adenosine stress in patients with ARVC. This hypothesis would be in line with the not completely blunted but significant decrease of about 30% in adenosine flow reserve in patients with ARVC as compared to controls observed in this study. In six patients with ARVC in this cohort, ^{123}I-MIBG SPECT was additionally available from clinical diagnostics, and in five of these patients a reduced tracer uptake in the inferoseptal region of the left ventricle on the MIBG scan 4 h after injection was present. Interestingly, the mean peak MBF under adenosine stress was severely reduced in the five patients with MIBG defects (MBF 2.64± 1.31 ml/min/g), whereas the single patient with normal MIBG uptake had a normal adenosine-triggered MBF response of 4.25 ml/min/g. This finding could support an association between sympathetic function and microvascular function in patients with ARVC, but obviously the group studied in parallel by MIBG-SPECT and $H_2{}^{15}O$ PET was far too small, so prospective larger scale studies on this topic are necessary.

Study limitations

The relatively small number of patients with a rare cardiac disease without left ventricular involvement enrolled in this

study, although well characterized and selected, might not have represented the wide spectrum of disease manifestation among patients with ARVC. Due to the limited spatial resolution of the PET scanner, quantitative perfusion measurements within the thin right ventricular wall were, and still are, impossible.

Conclusion

In conclusion, this study demonstrated an impairment of MBF and hyperaemic flow reserve associated with an increase in minimal coronary resistance in male patients with ARVC.

Acknowledgments This study was supported by the Deutsche Forschungsgemeinschaft, Sonderforschungsbereich SFB 656 (projects A1, C1 & C6), Münster, Germany.

Conflicts of interest None.

References

1. Marcus FI, McKenna WJ, Sherrill D, Basso C, Bauce B, Bluemke DA, et al. Diagnosis of arrhythmogenic right ventricular cardiomyopathy/dysplasia: proposed modification of the task force criteria. Circulation. 2010;121:1533–41.
2. Paul M, Wichter T, Kies P, Gerss J, Wollmann C, Rahbar K, et al. Cardiac sympathetic dysfunction in genotyped patients with arrhythmogenic right ventricular cardiomyopathy and risk of recurrent ventricular tachyarrhythmias. J Nucl Med. 2011;52:1559–65.
3. Neglia D, Michelassi C, Trivieri MG, Sambuceti G, Giorgetti A, Pratali L, et al. Prognostic role of myocardial blood flow impairment in idiopathic left ventricular dysfunction. Circulation. 2002;105:186–93.
4. Cecchi F, Olivotto I, Gistri R, Lorenzoni R, Chiriatti G, Camici PG. Coronary microvascular dysfunction and prognosis in hypertrophic cardiomyopathy. N Engl J Med. 2003;349:1027–35.
5. Lang RM, Bierig M, Devereux RB, Flachskampf FA, Foster E, Pellikka PA; American Society of Echocardiography's Nomenclature and Standards Committee; Task Force on Chamber Quantification; American College of Cardiology Echocardiography Committee; American Heart Association; European Association of Echocardiography, European Society of Cardiology, et al. Recommendations for chamber quantification. Eur J Echocardiogr. 2006;7:79–108.
6. Range FT, Schäfers M, Acil T, Schäfers KP, Kies P, Paul M, et al. Impaired myocardial perfusion and perfusion reserve associated with increased coronary resistance in persistent idiopathic atrial fibrillation. Eur Heart J. 2007;28:2223–30.
7. Schäfers KP, Spinks TJ, Camici PG, Bloomfield PM, Rhodes CG, Law MP, et al. Absolute quantification of myocardial blood flow with H(2)(15)O and 3-dimensional PET: an experimental validation. J Nucl Med. 2002;43:1031–40.
8. Campisi R, Czernin J, Schöder H, Sayre JW, Marengo FD, Phelps ME, et al. Effects of long-term smoking on myocardial blood flow, coronary vasomotion, and vasodilator capacity. Circulation. 1998;98:119–25.
9. Buus NH, Bøttcher M, Hermansen F, Sander M, Nielsen TT, Mulvany MJ. Influence of nitric oxide synthase and adrenergic inhibition on adenosine-induced myocardial hyperemia. Circulation. 2001;104:2305–10.
10. Feigl EO. Neural control of coronary blood flow. J Vasc Res. 1998;35:85–92.
11. Wichter T, Schäfers M, Rhodes CG, Borggrefe M, Lerch H, Lammertsma AA, et al. Abnormalities of cardiac sympathetic innervation in arrhythmogenic right ventricular cardiomyopathy: quantitative assessment of presynaptic norepinephrine reuptake and postsynaptic beta-adrenergic receptor density with positron emission tomography. Circulation. 2000;101:1552–8.